Malaysian
Journal Of Civil
Engineering

Full Paper

CORROSION BEHAVIOR OF REINFORCING STEEL IN RC SLAB CONTAINING CHLORIDES WITH PARTIAL REPLACEMENT OF CEMENT AS FLY ASH

Sristi Das Gupta[a*], Takafumi Sugiyama[b] , Md Shafiqul Islam[a]

[a]Department of Civil Engineering, Faculty of Engineering, Ahsanullah University of Science and Technology, Tejgao, Dhaka, Bangladesh
[b]Department of Civil Engineering, Faculty of Engineering, Hokkaido University, Sapporo, Hokkaido, Japan

Article history
Received
15 August 2019
Received in revised form
13 October 2019
Accepted
27 October 2019
Published online
30 November 2019

*Corresponding author
sristi.ce@aust.edu

Abstract

Steel reinforcement in concrete containing fly ash has been practically employed to RC structures in snowy cold region and coastal areas so that the durability of the structures against corrosion can be enhanced. In this research to make the compatibility with RC slab bridge sodium chloride solution of 10% in concentration was applied on RC slab and corrosion development was monitored by electrochemical method. Applying fly ash in RC slab at two replacement levels of 15% (F15) and 30% (F30) of cement the specimens were observed. The observation result verified that fly ash concrete showed longer period of corrosion initiation (ASTM C876) than normal reinforced concrete. The initiation period of corrosion was 4.5 and 6 times longer for F15 and F30 concrete than normal concrete, as well as 91 days strength of F30 concrete was about 14% higher that of norma concrete. Test result showed that fly ash has better influence on steel corrosion reduction than concrete cover increment. It was observed that fly ash concrete (F15 and F30) with 3 cm concrete cover has better corrosion resistivity than using 4 cm cover of non-fly ash concrete. Furthermore, using the same concrete cover (3 cm) it was found that the actual corrosion rate was decreased about 68 to 82% by adding fly ash 15 to 30% respectively compared to normal reinforced concrete. In addition, a significant attenuation in corrosion area in rebar between fly ash concrete and normal concrete was found. Based on actual corrosion area on rebar surface, actual corrosion current density was larger than corrosion current density found from non-destructive way. Moreover, further analysis was conducted for characterization of different corrosion products using Raman spectroscopy with 532 nm wave length. It revealed that the corrosion product (Oxides and Oxyhydroxides compound) were less in F15 and F30 concrete compared to normal concrete. Considering these results, the possibility of reduction of chloride induced corrosion in reinforced concrete structure using fly ash has confirmed.

Keywords: Chloride concentration, Concrete; Corrosion, Fly ash, Oxides and Oxyhydroxides, Raman spectroscopy;

1.0 INTRODUCTION

Corrosion of steel reinforcement in concrete is the most predominant problem affecting the serviceability and safety of reinforced concrete structure. Reinforcing bars in concrete with high alkaline ambience can form oxidized passive film, which can separate water and oxygen from reinforcement to prevent corrosion. The protective passive film breaks down with the ingression of chloride into the concrete which deteriorates the long-term performance of reinforced concrete structure. The penetration of chlorides into reinforced concrete occurs by various transport mechanisms depending on the exposure conditions. For instances, in many countries the use of de-icing salts (6~10%) to combat the build-up snow during the winter months on transport infrastructures causes the degradation of bridges, support columns, parking garages, and other steel-reinforced concrete structures. Since corrosion is an electrochemical process, resistivity of chloride penetration which in terms depend of permeability of concrete is the key to overall durability. The permeability of concrete is mainly dependent on the type of cement and other mix constituents, concrete mix proportions, compaction and curing. Incorporating mineral admixture such as, fly ash, silica fume can reduce the permeability of concrete and shows good resistance against chloride penetration and corrosion of steel reinforcement. Fly ash, which contains high alumina content, activate robustly pozzolanic reactions with the cement resulting in the formation of a greater and denser calcium silicate hydrate (CSH) structure and tricalcium-aluminate (C_3A), capable of chemically binding chloride ions. In addition, presence of carbon in fly ash stymie the strength development in concrete at early ages. However, after 28 days concrete contains fly ash have ameliorated strength that surpasses non-fly ash concrete mixes. After corrosion initiation the de-passivation of steel rebars can lead to the localized formation of iron oxide and hydroxides layers at the steel-concrete interface. The damage of concrete produced by corrosion will depend on the types of corrosion products presence within the reinforced concrete. Therefore, the study and characterization of corrosion products in reinforced concrete is an important issue to measure the corrosion state within RC structure. According to Chitty et al. (2005) corrosion system was made up of a multilayer structure constituted of a dense corrosion product layer (DPL). Dense Product Layer is mainly made of iron oxi-hydroxides (goethite, lepidocrocite and akaganeite) and iron oxides (maghemite and magnetite) [1]. "Lepidocrocite (γ-FeOOH) plays an important role in the corrosion mechanism" [5]. It is mainly developed in the initial stage of corrosion, when iron oxi hydroxides in the presence of aggressive impurities (the amount of chloride present in the steel surface) transform into lepidocrocite product. Therefore, the concentration of chloride ions influenced the nature of iron phase.

Since several oxyhydroxides and hydroxides can be formed as corrosion product it is significant to ascertain if they become from laser exposure to radiation transformation or as corrosion products.

Research with initiation of corrosion as well as chloride diffusion rate in reinforced concrete slab had been already noticed. Compared to that research, this manuscript can provide the more detail information regarding corrosion current, actual corrosion area with different w/c ratio, relation between chloride concentration and corrosion current as well as most significantly corrosion products detection using raman spectrometer with excitation wavelength 532 nm and a laser power of 2mW and variation between normal RC slab and fly ash concrete slab using 15% and 30% cement replacement. Moreover, the performance of fly ash against corrosion of reinforced concrete structure is also presented in the paper. As maintenance, construction, designing and protection of reinforced concrete structures are the most important requirements, the significances of these supplementary materials are needed to be intensively studied for reinforced concrete construction.

2.0 MATERIALS AND METHODS

2.1 Materials

2.1.1 Cement

Ordinary Portland cement was used in this research. Standard specifications of OPC according to JIS are shown in Table 1.

Table 1 JIS standard specification of OPC

Item		JIS * Standards (JIS R 5210)
Specific Surface Area (cm^2/g)		More than 2500
Setting	Initial Set h-min Final Setting h-min	More than 60min Less than 10h
Compressive Strength (N/mm^2)	28d	More than 42.5

2.1.2 Fly Ash

Historically, fly ash has been used in concrete at levels ranging from 15% to 50% by mass of the cementitious material component. However, several researches [15] have demonstrated that as the fly ash content increases, the development of pozzolanic reactions decreases because there is not enough calcium hydroxide in the system to react with all of the available fly ash, which in turn leads to the development of a porous microstructure. Moreover, at high levels structure may encountered with extended set times and slow strength development, delays the corrosion initiation process which would hinder the actual goal of the research. Considering these drawbacks in this research fly ash concrete was produced by incorporating minimum (15%) to medium (30%) level of Fly ash to analyze the corrosion process. According to JIS standard fly ash as used in this study is categorized as type II in which SiO_2 contents are 68%.

2.1.3 Aggregates

Crushed sand was used as fine aggregate while crushed stone conforming to JIS A 5005 was used as coarse aggregate. A 20 mm nominal size stone was used for experimental work.

2.1.4 Reinforcing Steel

The reinforcing steel (working electrode) used for corrosion tests was deformed steel bar with a diameter of 19 mm.

2.1.5 Air Content

The air content in concrete was 4.7-4.8% of the concrete volume depending on the maximum size of coarse aggregate in accordance with JIS A1116.

2.2 Concrete Mix Proportions

In the laboratory as per ACI 211.1-91 [20] to achieve the intended slump of 9.5 cm for RC slab, trial immixture was carried so that concrete could meets the mix proportion requirements. A sum of 30 specimens with 6 groups were made (e.g. NA, NB, F15A, F15B, F30A, F30B). Normal concrete with type A (NA) and type B(NB), Fly ash concrete with 15% cement replacement type A (F15A) and type B (F15B), Fly ash concrete with 30% cement replacement type A (F30A) and type B (F30B), Dimensions of type A, type B specimen were respectively 100X128X300 mm (Fig.1b) and 100X148X300 mm (Fig.1b) where fly ash concrete produced by supplanting 15% (F15) and 30% (F30) of OPC with fly ash. Every specimen contains two longitudinal reinforcements in which reinforcement with 30 mm cover distance from top surface named as up rebar and 30 mm cover distance from bottom surface named as bottom rebar. After casting specimens were cured for 28 days and 91 days for strength test. However, various w/c ratios were used for normal and fly ash concrete to keep up the same slump (9.5 cm), it was found that 91 days strength of fly concrete mixes surpassed normal concrete mixes. After achieving desired strength an acrylic canister dimensioning 50 mm X100 mm in cross section was introduced for NaCl solution of 10% in concentration [11] (Figure 1a). Detailed mix proportions of constituent materials to produce concretes are presented in Table 2.

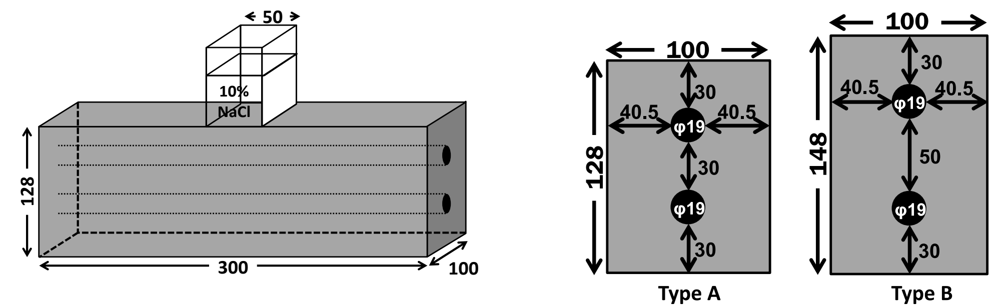

(a) (b)

Figure 1 (a) RC slab with 10% NaCl solution on top; (b) RC slab of type A (100X128X300 mm) and type B (100X148X300 mm) specimen [19]

Table 2 Concrete mix proportions used in the study.

Type	G_{max} (mm)	Slump (cm)	Air (%)	W/ (C+FA) (%)	Unit weight (kg/m³)					Strength (N/mm²)	
					W	C	FA	S	G	28 Days	91 Days
N	20	9.5	4.7	63.5	142	224	0	1,002	995	30.2	33.3
F15	20	9.5	4.8	58.5	132	192	34	969	1042	28.1	33.9
F30	20	9.5	4.8	49.5	126	178	76	919	1071	29.6	37.5

2.3 Corrosion Current Density Measurement

Monitoring of corrosion was done by half-cell potential method and polarization resistance method. After fruitful detection of corrosion, the specimens were carved and divided to visualize corrosion. Rebar corrosion area was measured followed by the cutting and splitting of corrosion test specimens. After cutting the corrosion test specimens, it was found that corrosion was initiated on the rebars vertically just below the chloride application zone as schematically presented in Fig.2a. The rebar was cut to a length of 9 cm (Fig.2a). An image of the corroded bar has been produced by which computer image analysis software (Image J) has been used to quantify the corrosion area (Fig.2b).

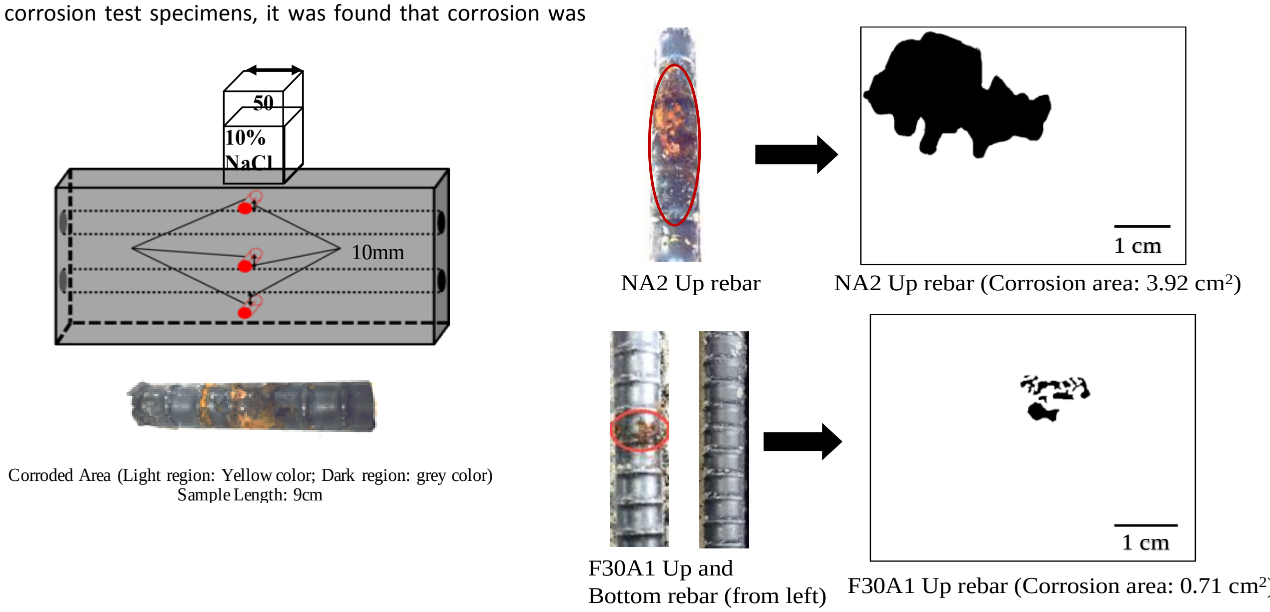

(a) (b)

Figure 2 (a) Concrete powder taken out from three different locations; (b) Rebar corrosion area (cm²) analyzed by 'Image J' software

2.4 Chloride Analysis

For the measurement of chloride concentration, 10 grams of concrete powder was taken out from three points in the near of up rebar and bottom rebar of the normal and fly ash concrete specimen of the entire chloride application zone (50mm x 100 mm) (Fig.2a). Thereafter, chloride ion concentration in each point of the specimen has been measured using an automatic chloride ion titration device (GT-100).

2.5 Corrosion Products Analysis by Raman Spectroscopy

To study the corrosion products formed on steel inserted in fly ash concrete a Raman spectrometer with wave length of 532 nm was used. The measurements were done directly in the sample with the sample length 9 cm (Fig.2). The Raman shift was calibrated before the measurements according to the silicon peak at 520 cm^{-1}. The 532-nm line had a laser power from 0.005% to 100% of laser power 2mW. The laser was set at 0.05 to 50% of the power. Moreover, for precise analysis, rebar corrosion area was divided in two regions. 'Dark region' for grey color of rebar corrosion and 'Light region' for yellow color of rebar corrosion (Fig.2a).

3.0 RESULTS AND DISCUSSION

3.1 Effect of Chloride Ion Concentration on Corrosion Current Density

For the F15 and F30, total of 6 fly ash concrete specimens (F15A2, F15B4, F30A1, F30A2, F30B2 and F30B4) and 10 normal concrete specimen showed corrosion initiation, based on ASTM C-876, in the presence of chlorides. The initiation period of F30 concrete was about 6 times longer than the normal concrete (N) as opposed to F15 concrete on which it was found about 4.5 times higher period of corrosion initiation than the normal concrete (N) (Fig. 3a). The longer period of corrosion initiation in UP rebar in fly ash concrete (F30) is due to diffusion of chloride ion in concrete to reach the rebar surface for initiation of corrosion takes longer time than normal concrete. A regression equation obtained between corrosion current and chloride concentration after corrosion initiation at different w/c ratios with concrete cover thicknesses are shown in Table 3.

A significant regression is obtained at w/c ratio of 0.635 (3 cm cover). This could be explained by the fact that this w/c ratio are more porous than the w/c ratios of 0.585 and 0.495 and corresponding the chloride penetration is higher. No significant regressions were obtained for the w/c ratio of 0.495 with 3 cm concrete cover the addition of 30% fly ash in concrete slab. While on the contrary, statistically significant regression equation was obtained (4 cm cover) for 0.4 w/c ratio [21]. Comparing with the regression equation, it can be summarized that by lowering w/c ratio and increasing concrete cover, corrosion current rate could not be significantly decreased while influence of fly ash can significantly decreases corrosion current rate without concrete cover increment.

Table 3 Summary of chloride concentration and corrosion current density for normal and fly ash concrete.

Cover (cm)	w/c (%)	R^2	Regression equation Ic (μAcm^{-2}) = a + b Cl	Cover* (cm)	w/c* (%)	R^{2*}	Regression equation* Ic (μAcm^{-2}) = a + b Cl
3	63.5	0.97	Ic = 0.43Cl+0.76	2	50	0.87	Ic = 0.56Cl+0.02
3 (15% fly ash)	58.5	0.82	Ic = 0.14Cl+0.13	4	60	0.74	Ic = 0.32Cl +0.05
3 (30% fly ash)	49.5	0.82	Ic = 0.07Cl+0.13	4	40	0.62	Ic = 0.19Cl+0.02

*Castaneda A, *et.al;* 2013

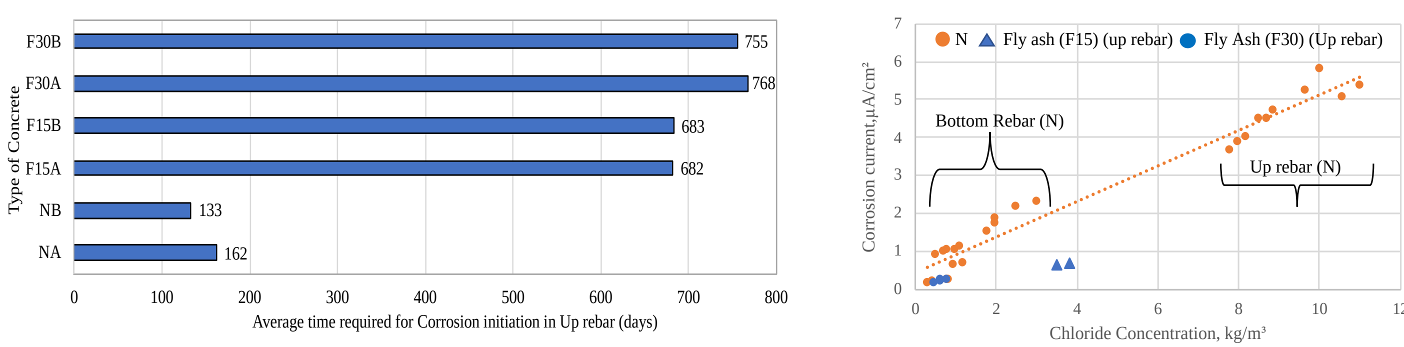

(a)

(b)

Figure 3 (a) Average corrosion initiation time of UP rebar in normal and fly ash concrete; (b) Relationship between Chloride concentration and corrosion current density for normal and fly ash concrete

In Figure 3b, lowest chloride concentration of up rebar of F30B4 concrete was found 0.47 kg/m³ compared to NA and NB concrete specimen. It is enumerated from the Figure 4 that with the increment of chloride concentration in fly ash concrete the rate of corresponding increment of corrosion current density is very low compared to normal reinforced concrete.

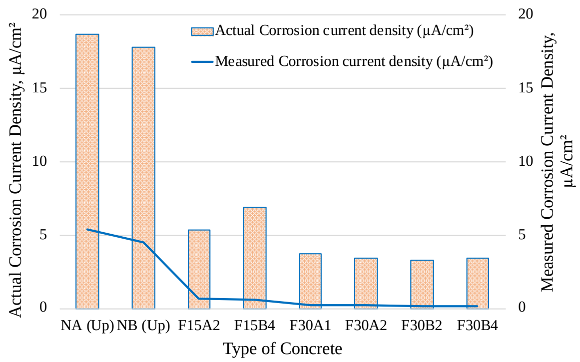

(a) Comparison of actual and measured corrosion current density

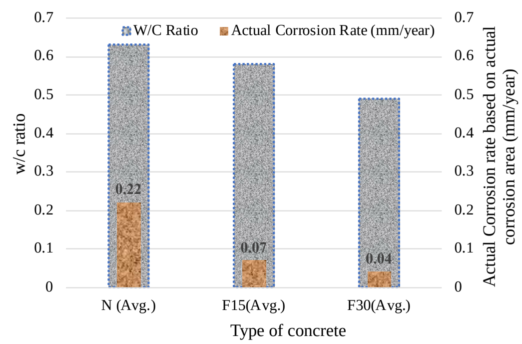

(b) Comparison of w/c ratio and actual corrosion rate based on actual corrosion area

Figure 4 Comparison of actual corrosion current density and actual corrosion current rate based on actual corrosion area of normal and fly ash concrete

Using actual corrosion area, it is seen from Figure 4(a) that both normal and fly ash concrete actual corrosion current density is higher than the measured current density. This is due to the fact that the measured corrosion area in the non-destructive method was normally larger than the actual area directly obtained in the destructive manner. Moreover, a comparison between w/c ratio and actual corrosion rate is also noticeable in figure 4(b). It is understandable that low w/c ratio will slow down the corrosion rate due to the presence of high amount of cement. Using the same concrete cover (3 cm) it was found that the actual corrosion rate was decreased about 68 to 82% by adding fly ash 15 and 30% with the replacement to cement compared to normal reinforced concrete (Figure 4b).

3.2 Corrosion Products of Normal and Fly ash Concrete

The study of corrosion products using Raman spectroscopy was located in a minuscule area (laser spot 4µm²). Based on color of rust (Yellow color: Light region; Grey color: Dark region) spectra for the light and dark regions obtained with a laser energy 532 nm and the variation of corrosion products in both dark and light region with the different chloride concentration are summarized in Table 4. Several researches *[5,6,7,8]* identified the phase of corrosion products of steel using Raman spectroscopy with a laser energy 532 nm. In this research detection of corrosion products using the peak of Raman intensity was based on previous research data *[5,6,7,8]* that are summarized on Table 4. Raman spectra of some of the normal and fly ash concretes are shown in Figure 5 to 7.

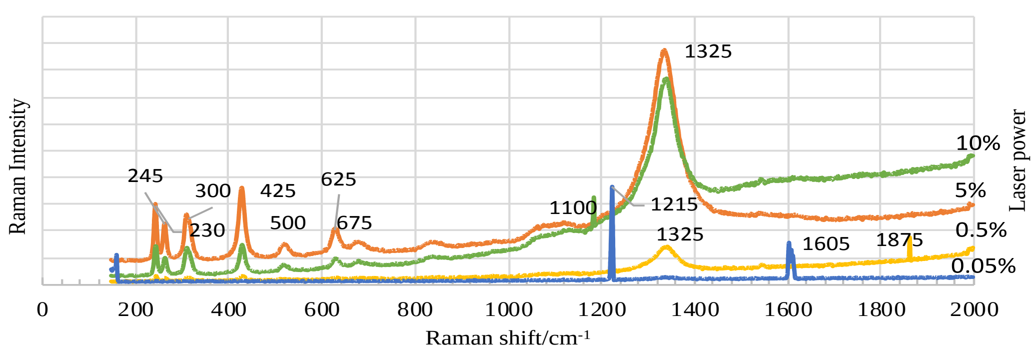

(a)

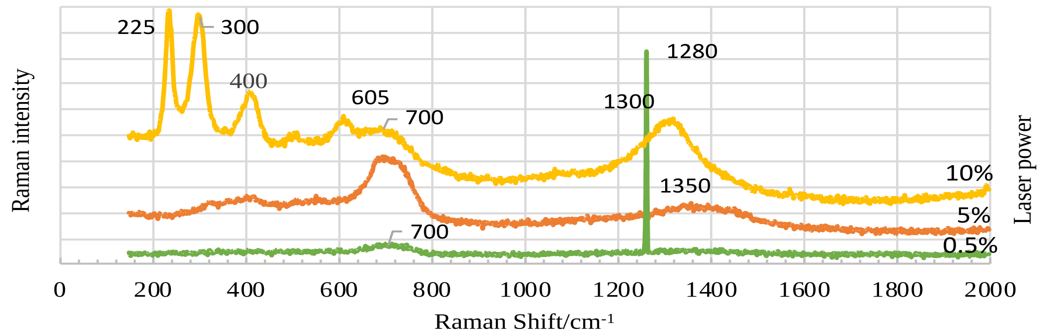

(b)

Figure 5 (a) Raman spectra for NA (4) Up Rebar (Dark Region); (b) NB (4) Up rebar (Light region)

Table 4 Corrosion products of fly ash concrete

Type of concrete	Name of specimen	Concrete cover (mm)	Chloride concentration on rebar surface (kg/m^3)	Identified phase Ref.no *[5,6,7,8]*	Corrosion products
N	NA	30(Up)	10.4	1595, 1300, 1100, 1035, 685, 625, 510, 395, 295, 230	G, L, H, Fh (*Dark region*)
		79(Down)	2.75	1315, 1100, 715, 600, 515, 410, 325, 295, 225	G, H, W, Fh, Mh (*Dark region*)
	NB	30(Up)	8.2	1325, 1285, 615, 545, 500, 415, 395, 300, 230	G, L, H, Mg, W Fh (*Dark region)*
				1595, 1300, 740, 595, 397, 296, 215	H, MH, W, O, L (*Light region*)
		99(Down)	0.78	1295, 700, 687, 395, 215	H, O, L (*Light region*)
F15	F15A2	30(Up)	2.31	1300,820,675, 525, 415,290	G, L, H, (*Dark region*)
	F15B4	30(Up)	1.84	1315,695, 415, 348	G, H, O (*Dark region*)
F30	F30A1	30(Up)	1.5	1600,710, 515, 355	Fh, Mh, (*Dark region*)
				1375, 755,530, 415, 300, 225	L, H (*Light region*)
	F30A2	30(Up)	1.4	1355,710, 425, 300,225	H, Fh, (*Dark region*)
				1595,740, 295, 225	H (*Light region*)
	F30B2	30(Up)	0.78	700	O (*Light region*)
	F30B4	30(Up)	0.55	700	O (*Light Region*)

Where, G-Goethite(α-FeOOH), L- Lepeidocrocite (γ-FeOOH), H-Hematite (α-Fe_2O_3), Mh-Meghemite (γ-Fe_2O_3), Mg-Magnetite (Fe_3O_4) Fh-Ferrihydrite, W-Wousite (FeO), O-iron Oxyhydroxide

From the Table 4, it has been seen that corrosion products are different in dark region and light region. This is mainly due to the difference in intensity of corrosion products. The dark region showed more substantial phase than the light region**.** In the Figure 5a, chloride concentration in up rebar of NA (4) is 9.4 kg/m^{3}and with that chloride concentration several peaks of geothite, lepidocrocite, hematite with ferrihydrite product were detected in the dark region. The intensity of peaks is wider and sharper with the increasing of laser power. On the other hand, in light region peaks of NA (4) iron oxyhydroxides, lepidocrocite and hematite products are identified. Spectra recorded in F15A2 (Fig.6) up rebar with 2.31 kg/m^3 chloride concentration a well-defined peak of Goethite, lepidocrocite and Hematite compounds were found.

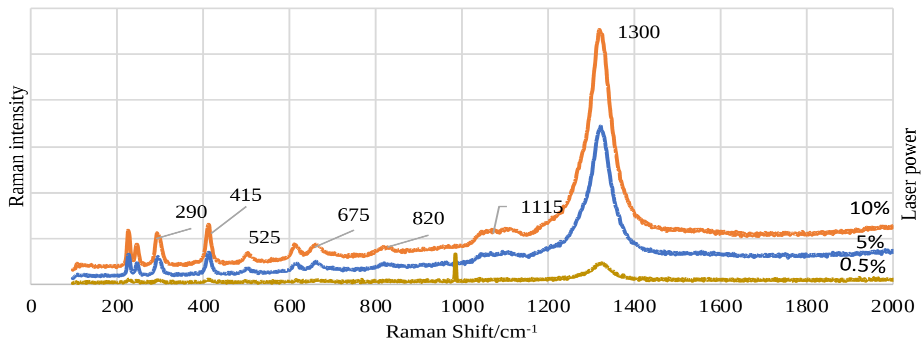

Figure 6 Raman spectra for F15A (2) Up rebar (Dark region)

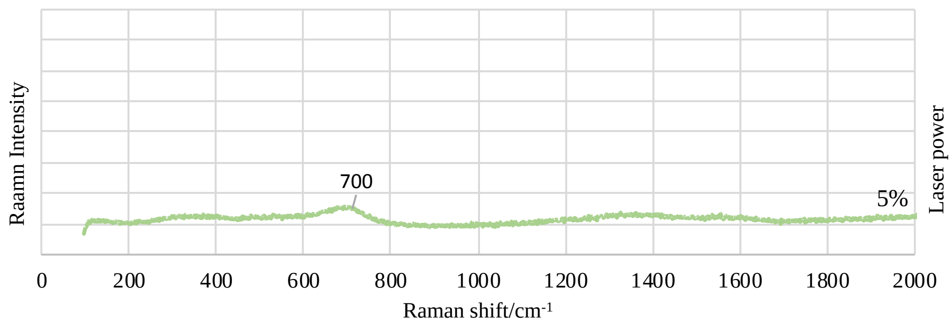

Figure 7 Raman spectra for F30B (2) Up rebar (Light region)

Regarding the influence of fly ash, it lessens the chloride ion mobility to the steel surface and abates the corrosion process. It is also cleared from the dependency of chloride concentration. In the F30B2 (Fig.7) and F30B4 series of fly ash concrete (Table 5), due to less chloride concentration from 0.78kg/m^3 to 0.55kg/m^3 only peak of iron oxyhydroxides with low raman intensity were detected.

Although the phenomenon for the variation of different iron oxide compound as a corrosion product in rebar surface is very complex, it can be recapitulated that presence of iron-oxide can vary with the color of corrosion. The difference in corrosion products in dark region and light region is mainly due to the color of rust in the dense corrosion product layer (DPL). The light region of DPL layer is less stable than dark region because of the presence of poor phase of iron oxyhyroxide (lepidocrocite) where in the dark region it includes strong goethite band with several iron oxides product. In all cases, the raman intensity of peak in light region is less stable than dark region. Regarding the influence of fly ash in concrete it was noticed that a modicum of corrosion products generated on the surface of steel embedded in F30 concrete, which were poorly phases of iron oxyhydroxides (O), lepidocrocite (γ-FeOOH), hematite (α-Fe_2O_3) and meghemite (γ-Fe_2O_3) whereas in F15 concrete strong goethite(α-FeOOH), iron oxyhydroxides (O), lepidocrocite (γ-FeOOH) and hematite (α-Fe_2O_3) were identified. Furthermore, neither Fe_3O_4 nor akaganeite were detected in all the fly ash specimen, indicated that the amount of chlorine was not enough in the DPL to stabilise this phase [5]. Because, to stabilize the dense corrosion product layer (DPL) it is required to present the goethite, lepidocrocite, akaganeite product with Iron oxides compound (magnetite, hematite) [1].

4.0 CONCLUSIONS

This paper reported experimental results of corrosion behavior of RC slab concrete incorporating of Fly ash. Based on this research, the following conclusions could be drawn;

- Fly ash concrete hardly manifests the initiation of the corrosion of the reinforcing steels in the RC slabs compared to normal concrete. After initiation of corrosion it is found that average corrosion initiation period of up rebar of F15 and F30 concrete was about 4.5 and 6 times longer than those of normal concrete.
- Fly ash has better influence on steel corrosion reduction than concrete cover. Test result showed that fly ash concrete (F15 and F30) with 3 cm concrete cover has better corrosion resistivity than using 4 cm cover of non-fly ash concrete. As well as the same concrete cover (3 cm) it was found that the actual corrosion rate was decreased about 68 and 82% by adding fly ash 15 and 30% respectively compared to normal reinforced concrete.
- A significant reduction in corrosion area in rebar between fly ash concrete and normal concrete was found. Based on actual corrosion area on rebar surface, actual corrosion current density was larger than corrosion current density found from non-destructive way.
- Different corrosion products were identified with different chloride concentrations for both normal and fly ash concretes. The type and intensity of corrosion products in F30 concrete were found fewer compared to F15 and normal reinforced concrete. Moreover, in normal reinforced concrete almost all iron oxyhdroxides (goethite, iron oxyhydroxides and lepidocrocite) and iron oxides (hematite, wusite, magnetite and

ferrihydrite) were found with high chloride concentrations.

- The corrosion products in dark region were disparate from those in light region and the intensity of peak in dark region was sharper than that of light region.
- Furthermore, in all cases F30 concrete shows greater resistivity against corrosion than F15 concrete.

Acknowledgements

The laboratory support provided by 'Environmental Material Engineering Laboratory' of Hokkaido University (Japan) is gratefully acknowledged.

References

[1] W.J. Chitty, P. Dillmann, V. L'Hostis and C. Lombard. 2005. Long-Term Corrosion Resistance Of Metallic Reinforcements In Concrete A Study Of Corrosion Mechanisms Based On Archaeological Artefacts. *Corrosion Science.* 47: 1555– 1581.

[2] Monika Hanesch. 2009. Raman Spectroscopy Of Iron Oxides And (Oxy) Hydroxides At Low Laser Power And Possible Applications In Environmental Magnetic Studies. *Geophysical Journal International.* 177: 941–948.

[3] S. D. Gupta and T. Sugiyama. 2017. Study on Corrosion of RC Slab with Partial Replacement of Cement as Fly Ash Using Non-destructive Testing Method, *8th Asia and pacific young researchers and Graduates Symposium (YRGS 2017)*, September 7-8, University of Tokyo, Japan.

[4] V. Talakokula, S. Bhalla, R.J. Ball, C.R. Bowen, G.L. Pesce, R. Kurchania, B. Bhattacharjee, A. Gupta and K. Paine. 2016. Diagnosis of Carbonation Induced Corrosion Initiation And Progression In Reinforced Concrete Structures Using Piezo-Impedance Transducers. *Sensors and Actuators A.* 242: 79-91.

[5] M. Criado, S. Martínez-Ramirez and J.M. Bastidas. 2015. A Raman Spectroscopy Study Of Steel Corrosion Products In Activated Fly Ash Mortar Containing Chlorides. *Construction and Building Materials.* 96: 383–390.

[6] D. Larroumet, D. Greenfield, R. Akid and J. Yarwood, 2007; Raman Spectroscopic Studies Of The Corrosion Of Model Iron Electrodes In Sodium Chloride Solution. *Journal of Raman Spectroscopy.* 38: 1577–1585.

[7] V. L'Hostis, E. Amblard, W. Guillot, C. Paris and L. Bellot-Gurlet 2013. Characterisation of the Steel Concrete Interface Submitted To Chloride-Induced-Corrosion. *Materials and Corrosion*. 64: 185–194.

[8] Peter J. Mohr, Barry N. Taylor and David B. Newell. 2006. Committee on Data for science and technology (CODATA), NIST, 2006. *CODATA Recommended values of the Fundamental Physical Constants*, http://physics.nist.gov/cuu/Constants/codata.pdf

[9] S.D. Gupta and T.Sugiyama, 2018. Study on Corrosion of Reinforcing Steel in Concrete Slab Containing Fly Ash, *International Conference on Research and Innovation in Civil Engineering (ICRICE 2018),* January 12-13, Southern University Bangladesh, Bangladesh.

[10] C. M. Hansson, A. Poursaee and S. J. Jaffer; 2012. Corrosion of Reinforcing Bar in Concrete, The Masterbuilder, www.masterbuilder.co.in. Access on December 2012

[11] Toyoaki Miyagawa, Ueda Tamon, Hiroshi Yokota and Sugiyama Takafumi. 2007. Standard Specification For Concrete Structures, *Japan Society of Civil Engineers (JSCE),* ISBN 978-4-8106-0753-6.

[12] Zafar and T. Sugiyama, 2014. Laboratory Investigation to Study the Corrosion Initiation of Rebars in Fly ash Concrete. *Magazine of Concrete Research.* 66(20): 1051-1064.

[13] Zafar and T. Sugiyama. 2014. Experimental Factors with regard to Increased Corrosion Resistance in Fly Ash Concrete. *EURO COAL ASH 2014*, October 14-15. Munich, Germany. 251-264.

[14] Zafar and T. Sugiyama. 2014. Study on the Corrosion of Rebars in Fly Ash Concrete during Moderate to High Corrosion Rate. "*Fourth International Symposium on Life-Cycle Civil Engineering, IALCCE 2014*", November 16-19, Waseda University, Tokyo, Japan. 1538-1543.

[15] Vysal M and Veysel A. 2012. Durability performance of concrete incorporating Class F and Class C fly ashes, *Construction and Building Materials*, 34: 170–178.

[16] Boga A R and BekirIlker T. 2012. Influence of Fly Ash On Corrosion Resistance And Chloride Ion Permeability Of Concrete. *Construction and Building Materials*. 31: 258–264.

[17] Shaikh F U and Supit S. 2015. Compressive strength and durability properties of high volume fly ash (HVFA) concretes containing ultrafine fly ash (UFFA), *Construction and Building Materials*. 82: 192–205

[18] Gurdian H.; Alcocel E.G.; Baeza-Brotons, F.; Garcés, P. and Zornoza, E 2014. Corrosion Behaviour of Steel Reinforcement in Concrete with Recycled Aggregates, *Fly Ash and Spent Cracking Catalyst Materials*. 7: 3176–3197.

[19] S. D. Gupta and M. M. Momo. 2019; Monitoring of Corrosion in Fly Ash Concrete Slab Containing Chlorides by Electrochemical Method, *Proc. 2nd International Conference on Structural Engineering Research (iCSER2019), ISBN: 978-0-6482681-2-3,* January 19-22, Dhaka, Bangladesh, 48-53.

[20] ACI 211.1, 2009. Standard Practice for Selecting Proportions for Normal, Heavyweight and Mass Concrete. American Concrete Institute. American Concrete Institute, Farmington Hills, MI, 48331-3439 USA.

[21] Castaneda A, Howland J J, Corvo F Perez T. 2013. Corrosion of Steel Reinforced Concrete In The Tropical Coastal Atmosphere of Havana city, Cuba. *Quim. Nova.* 36(2): 220-229.